Remote Sensing of Environment 154 (2014) 61–73

Contents lists available at ScienceDirect

Remote Sensing of Environment

journal homepage: www.elsevier.com/locate/rse

Improving estimates of forest disturbance by combining observations from Landsat time series with U.S. Forest Service Forest Inventory and Analysis data

Todd A. Schroeder [a,*], Sean P. Healey [a], Gretchen G. Moisen [a], Tracey S. Frescino [a], Warren B. Cohen [b], Chengquan Huang [c], Robert E. Kennedy [d], Zhiqiang Yang [e]

[a] U.S. Department of Agriculture Forest Service, Rocky Mountain Research Station, Ogden, UT 84401, USA
[b] U.S. Department of Agriculture Forest Service, Pacific Northwest Research Station, Corvallis, OR 97331, USA
[c] Department of Geography, University of Maryland, College Park, MD 20742, USA
[d] Department of Earth & Environment, Boston University, Boston, MA 02215, USA
[e] Department of Forest Ecosystems and Society, Oregon State University, Corvallis, OR 97331, USA

ARTICLE INFO

Article history:
Received 20 March 2014
Received in revised form 4 August 2014
Accepted 6 August 2014
Available online 6 September 2014

Keywords:
Forest disturbance
Design-based estimation
Disturbance mapping
Post-stratification
Landsat time series
Forest Inventory and Analysis (FIA)

ABSTRACT

With earth's surface temperature and human population both on the rise a new emphasis has been placed on monitoring changes to forested ecosystems the world over. In the United States the U.S. Forest Service Forest Inventory and Analysis (FIA) program monitors the forested land base with field data collected over a permanent network of sample plots. Although these plots are visited repeatedly through time there are large temporal gaps (e.g. 5–10 years) between remeasurements such that many forest canopy disturbances go undetected. In this paper we demonstrate how Landsat time series (LTS) can help improve FIA's capacity to estimate disturbance by 1.) incorporating a new, downward looking response variable which is more sensitive to picking up change and 2.) providing historical disturbance maps which can reduce the variance of design-based estimates via post-stratification. To develop the LTS response variable a trained analyst was used to manually interpret 449 forested FIA plots located in the Uinta Mountains of northern Utah, USA. This involved recording cause and timing of disturbances based on evidence gathered from a 26-year annual stack of Landsat images and an 18-year, periodically spaced set of high resolution (~1 m) aerial photographs (e.g. National Aerial Image Program, NAIP and Google Earth). In general, the Landsat data captured major disturbances (e.g. harvests, fires) while the air photos allowed more detailed estimates of the number of trees impacted by recent insect outbreaks. Comparing the LTS and FIA field observations, we found that overall agreement was 73%, although when only disturbed plots were considered agreement dropped to 40%. Using the non-parametric Mann–Whitney test, we compared distributions of live and disturbed tree size (height and DBH) and found that when LTS and FIA both found non-stand clearing disturbance the median disturbed tree size was significantly larger than undisturbed trees, whereas no significant difference was found on plots where only FIA detected disturbance. This suggests that LTS interpretation and FIA field crews both detect upper canopy disturbances while FIA crews alone add disturbances occurring at or below canopy level. The analysis also showed that plots with only LTS disturbance had a significantly greater median number of years since last FIA measurement (6 years) than plots with both FIA and LTS disturbances (2.5 years), indicating that LTS improved detection on plots which had not been field sampled for several years. Next, to gauge the impact of incorporating LTS disturbances into the FIA estimation process we calculated design-based estimates of disturbance (for the period 1995–2011) using three response populations 1.) LTS observations, 2.) FIA field observations, and 3.) Combination of FIA and LTS observations. The results showed that combining the FIA and LTS observations led to the largest and most precise (i.e. smallest percent standard error) estimates of disturbance. In fact, the estimate based on the combined observations (486,458 ha, +/−47,101) was approximately 65% more than the estimate derived solely with FIA data (294,295 ha, +/−44,242). Lastly, a Landsat forest disturbance map was developed and tested for its ability to post-stratify the design-based estimates. Based on relative efficiency (RE), we found that stratification mostly improved the estimates derived with the LTS response data. Aside from insects (RE = 1.26), the estimates of area affected by individual agents saw minimal gain, whereas the LTS and combined FIA + LTS estimates of total

* Corresponding author. Tel.: +1 801 625 5690.
E-mail address: tschroeder@fs.fed.us (T.A. Schroeder).

http://dx.doi.org/10.1016/j.rse.2014.08.005
0034-4257/Published by Elsevier Inc.

disturbance saw modest improvement, with REs of 1.43 and 1.50 respectively. Overall, our results successfully demonstrate two ways LTS can improve the completeness and precision of disturbance estimates derived from FIA inventory data.

Published by Elsevier Inc.

1. Introduction

In addition to being one of the primary drivers of the net terrestrial carbon budget (Harmon, 2001; Kasischke et al., 2013), forest disturbance also plays a critical role in affecting biodiversity (Dornelas, 2010), wildlife habitat (Gibson et al., 2013) and the surface energy balance (O'Halloran et al., 2011). With rising global temperatures (Easterling et al., 2000; IPCC, 2014) and an ever growing human population (Raftery, Li, Ševčiková, Gerland, & Heilig, 2012) poised to alter the frequency and severity of disturbance regimes across the globe (Bradford, Jensen, Domke, & D'Amato, 2013; Dale et al., 2001; Westerling, Hidalgo, Cayan, & Swetnam, 2006), improved monitoring of forest disturbance, especially at the landscape scale has become increasingly important. Because forest disturbance manifests at a variety of spatial and temporal scales (Asner, 2013) and has varying impacts which affect the canopy, understory and forest floor, effective monitoring will likely require a hybrid approach, where detailed field measurements collected in a probabilistic sample are combined with frequent, repeated observations made by remote sensing satellites.

In the United States, the Forest Service Forest Inventory and Analysis (FIA) program (http://www.fia.fs.fed.us/) collects detailed field measurements which are used to produce timely and accurate estimates of a wide range of forest attributes. These attributes, which include forest area and volume, are used to provide information on the current status and health of forests over varying geographical extents. Typically, a probabilistic sample of inventory plots is used to estimate amount of forest area while maps derived from remote sensing have been used both as strata applied to reduce variance (i.e. for "post-stratification", see McRoberts, Wendt, & Liknes, 2005) and to delineate forest location and extent (McRoberts & Tomppo, 2007). Reporting population estimates at the state and county level has long been a primary function of FIA. However, with increasing stress on forested ecosystems (van Mantgem et al., 2009; Weed, Ayres, & Hicke, 2013), a new emphasis has been placed on improving FIA's capacity to report on how much forest is changing, where it is changing and what is changing it. This includes developing a flexible monitoring system which can estimate annual trends, report on different geographic areas (e.g. administrative units, watersheds, or ecoregions), as well as incorporate different spatial layers for use in post-stratified variance reduction.

Presently, monitoring the status and trends of forest disturbance can be challenging for inventory programs as they often have long temporal gaps (e.g. several years to decades) between plot measurements. For example, in the western U.S., a 10 year cycle of measurements is required for the network of FIA plots to fully sample the entire forested landscape. Since forest disturbance and recovery dynamics vary irregularly (annual rates < 3% per year; Masek et al., 2013) over space and time, both the frequency (time) and spatial coverage (space) of observation determine how well a sample captures a rare event like disturbance (Patterson & Finco, 2011). Therefore, it would greatly benefit FIA if all of its plots could be monitored and updated annually, thus providing estimates of disturbance which better reflect the current condition of the forest landscape. This would be especially beneficial in the western states, where annual updating would give FIA better capacity to track and respond to episodic insect outbreaks and fires. Based on this need, there is potential for FIA to improve its change monitoring capabilities by incorporating more frequent observations from optical remote sensing satellites such as Landsat.

With a 40+ year historical archive and a 16 day repeat cycle, Landsat imagery offers an excellent data source for monitoring forest disturbance over large areas (Hansen & Loveland, 2012). The 30 m spatial grain and 6 reflective bands are capable of capturing many types of forest disturbance, especially those that impact the upper canopy (Cohen & Goward, 2004). Now that the entire Landsat archive is freely available it has become economically feasible to monitor disturbance over large areas using satellite time series. The increased accessibility of Landsat data has led to the emergence of several new automated algorithms which are capable of mapping historical disturbance using the spectral response from multiple image dates (Huang et al., 2010; Jin et al., 2013; Kennedy, Yang, & Cohen, 2010; Zhu, Woodcock, & Olofsson, 2012). Thanks in part to greater access to supercomputers such as the NASA Earth Exchange (NEX, https://nex.nasa.gov/nex/), these algorithms are now being run over increasingly larger areas (Hansen et al., 2013). For example, the North American Forest Dynamics (NAFD) project (Goward et al., 2008; Masek et al., 2013) is currently using the Vegetation Change Tracker (VCT, Huang et al., 2010) algorithm to produce a wall-to-wall forest disturbance map for the conterminous U.S. With the availability of Landsat-based disturbance maps on the rise, it is important to determine their utility for improving the precision of FIA estimates through post-stratification.

In addition to stratification, Landsat data have also recently emerged as an effective backdrop for collecting plot-level reference information on disturbance and land cover change. Visualization tools such as TimeSync (Cohen, Yang, & Kennedy, 2010) demonstrate how a trained analyst can use the spectral and temporal information from Landsat along with other spatial data to record timing and cause of most natural and anthropogenic disturbance events. Such ancillary data include high spatial resolution photos from NAIP and Google Earth; fire polygons from Monitoring Trends in Burn Severity (MTBS, www.mtbs.gov; Eidenshink et al., 2007); and disturbance grids compiled by the Landfire program (www.landfire.gov; Vogelmann et al., 2011). Because of Landsat's long historical record, the analyst interpretation approach has surfaced as one of the best (and only) methods for collecting reference data over the full range (20–40 years) and interval (annual) of most time series maps. In addition to validation, analyst-based LTS observations can also be used for design-based estimation if collected over a statistically-based set of sample locations such as FIA plots. In fact, it is possible that combining the improved frequency and spatial coverage of LTS observations with the detailed, but less frequently acquired FIA field data might provide the most complete picture of where and how disturbance is impacting the greater landscape. In general, combining LTS and field-based observations in a design-based framework is an emerging technique for estimating (or predicting) landscape scale disturbance dynamics (e.g. see Plugmacher, Cohen, Kennedy, & Yang, 2014) and for validating maps of disturbance (Olofsson, Foody, Stehman, & Woodcock, 2013). Although our focus here is on FIA data, it is important to recognize that LTS observations, both in the form of maps and analyst-interpretations can be similarly applied to other sets of probabilistically collected field measurements.

Traditionally, Landsat data and its derivatives (e.g. National Land Cover Dataset, NLCD) have been used by FIA for post-stratification, a statistical technique for using spatial data to reduce the variance of design-based parameter estimates (McRoberts, Tomppo, & N sset, 2010). The literature suggests that static parameters such as forest area and volume have typically gained the greatest benefit from stratification (McRoberts et al., 2006; Nelson, McRoberts, Liknes, & Holden, 2002), while dynamic parameters reflecting forest change (e.g. growth, mortality and removals) have had much more limited success (Brooks, Coulston, Wynne, & Thomas, 2013; Gormanson, Hansen, & McRoberts, 2003). It is possible that stratification (which is based on agreement between map and sample plots) could improve if the FIA response variable

were measured annually over the full landscape and if a satellite disturbance map could be developed which accurately captures the prevailing disturbance dynamics of a region (e.g. agents and severity).

Therefore, the two main objectives of this study are to: 1.) Use LTS disturbance observations to augment FIA plots and determine how supplemental plot histories impact design-based estimates of disturbance, and 2.) Determine whether a Landsat disturbance map can improve (i.e. increase precision of) design-based estimates through post-stratified variance reduction. To address these objectives, we first use an analyst-led LTS interpretation approach (similar to TimeSync, Cohen et al., 2010) to collect supplemental disturbance history information on 449 forested FIA plots located in the Uinta Mountains of northern Utah, USA. In addition to annual Landsat imagery, a time series of high spatial resolution air photos from NAIP and Google Earth are used to expand the interpretation approach to include detailed tree-level measurements of mortality occurring below the resolution of the Landsat data. To better understand how the LTS and field observations relate to one another we use the cells of an agreement matrix to divide the plots into 3 disturbance populations (e.g. 1.) Both LTS and FIA find disturbance, 2.) Only FIA finds disturbance and 3.) Only LTS finds disturbance) which are used to compare distributions of live and disturbed tree size (i.e. height, HT and diameter at breast height, DBH) and number of years between LTS and FIA measurements using non-parametric Mann–Whitney tests. Next the FIA and LTS observations of disturbance are used individually and combined together to generate design-based estimates of disturbed area (for the period 1995–2011) for specific agent classes (e.g. insect, disease, fire, harvest, weather, mechanical, and animal) and their total. To test the potential for improving the precision of the derived estimates through post-stratification, we use a multi-stage approach to develop a Landsat forest disturbance map which better captures the subtle, low magnitude spectral changes associated with recent insect outbreaks. We evaluate the maps' capacity to increase the precision of the plot-based estimates using the measure of relative efficiency (RE = variance from simple random sampling/variance from post-stratification; see McRoberts, Holden, Nelson, Liknes, & Gormanson, 2006), which can be interpreted as the factor by which the size of a simple random sample would have to increase by to achieve the same precision as stratification. Testing the capacity of remote observations to improve disturbance estimates over a broad range of forest types and causal agents may provide a template for future integration of field and LTS observations within FIA's monitoring and reporting system.

2. Methods

2.1. Study area

The 1.6 million ha study area consists of the non-overlapping portion (or Thiessen Scene Area, TSA) of Landsat scene path 37 row 32, which covers nearly the entire Uinta Mountain range located in the northeast corner of Utah, USA (Fig. 1). Approximately 56% of the study area is forested including broad expanses of conifer and mixed deciduous forest, as well as stands of pure aspen at high elevations and sparse Pinyon-Juniper woodlands on drier, lower elevation slopes. According to the most recent US Forest Service forest type map (Ruefenacht et al., 2008) the majority of forest within the study area falls in 5 major group types. These include Pinyon-Juniper (18%), Aspen/Birch (12%), Fir/Spruce/Hemlock (12%), Lodgepole Pine (10%) and Douglas-fir (3%) (see Fig. 1). The diversity of forest types and land management objectives in the region have resulted in a wide array of disturbance agents, including harvests, fires, insects, and mechanical treatments such as chaining. Due in part to warmer winter temperatures and shifting precipitation patterns (Bentz et al., 2010; Hebertson & Jenkins, 2008), the Uinta Mountains have recently (i.e. 2004–2011) experienced elevated levels of mortality from insects such as mountain pine beetle and spruce beetle (DeBlander, Guyon, Hebertson, Mathews, & Keyes, 2012; Man, 2012). Given the broad array of disturbance agents which have occurred in both dense and sparse forest types the Uinta Mountains provide an excellent and challenging location to evaluate the expanded use of LTS observations within FIA's estimation process.

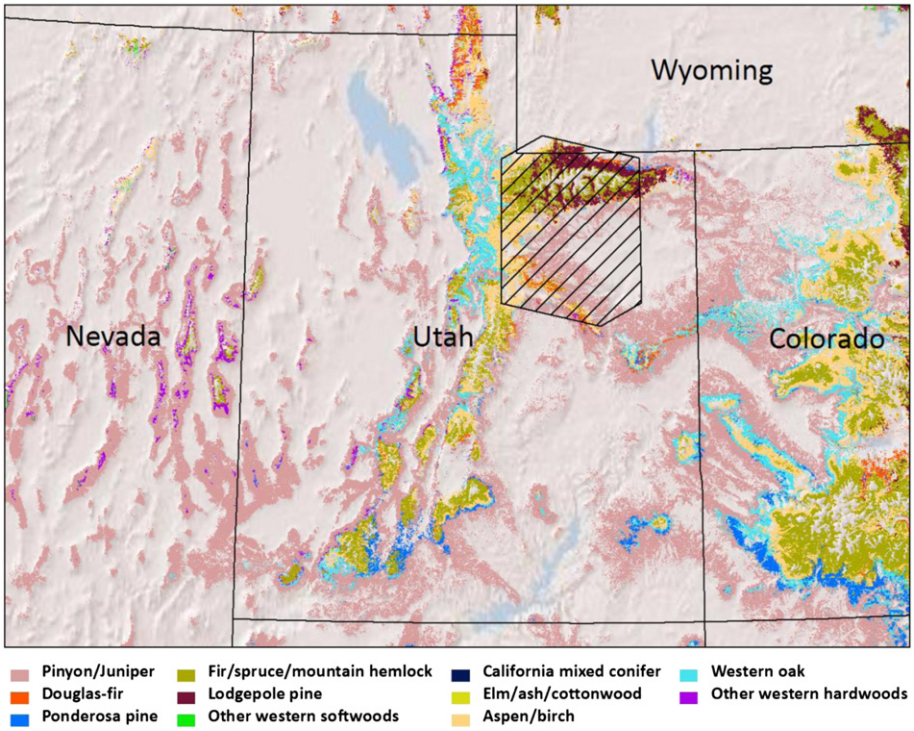

Fig. 1. The Uinta Mountains study area defined by the Landsat path 37 row 32 Thiessen scene area (TSA). Non-forest areas are shown in gray.

2.2. Data

2.2.1. FIA field disturbance observations

The field data used in this study consists of 790 phase 2 (P2) FIA plots (449 are forest; 341 non-forest) measured between 2000 and 2011. Part of FIA's annual inventory design (Reams et al., 2005), the P2 field plots are randomly located across the US on a hexagonal sampling frame at a density of 1 plot per 2403 ha (5937 acres). Sample trees are measured on four 7.32 m (24 ft) fixed radius subplots which together cover a 687.97 m^2 area (0.17 acres). It is important to note that at the plot-level FIA tree measurements come from the four subplots, which in total cover an area 1/6 of the size of the LTS photo plot (described below). In the western states, FIA measures plots on a 10 year rotating panel system such that 10% of all plots are measured annually. Therefore the data used here includes one full cycle of observations (i.e. all plots have been measured once), with an additional 20% having been measured twice during the period of study. During field visits, FIA crews collect a variety of forest attributes (e.g. forest type and disturbance) which are reported by condition classes reflecting distinct differences in land use or vegetation types found on a plot. Thus, it is possible for a plot to contain multiple forest conditions or a combination of forest and non-forest conditions. Both single- and multiple-condition plots were used in this study. For each plot the proportion of each condition is accounted for by an expansion factor (e.g. Trees per Acre) which is applied during the estimation process. Except for rare situations, field measurements (including observations of disturbance) are only collected on plots which potentially meet FIA's definition of "forest" (i.e. land which is at least 10% stocked with trees, or formerly had such tree cover and is not currently developed for a non-forest use). Here a binary labeling system is used to partition the forested FIA plots into disturbed and undisturbed categories based on information taken from both the condition and tree-level data.

At the condition-level, FIA crews record the timing of disturbances (e.g. insect, disease, fire, weather, animal, and other) and treatments (e.g. harvesting, from here on referred to as a disturbance) which are at least 4047 m^2 (1 acre) in size and that have significant mortality or damage to at least 25% of trees. Detecting and labeling disturbance from the ground perspective requires field crews to interpret the current ecological condition of the forest to identify and back-date the timing of past disturbance events. Since crews must look back 5 years during initial plot installation and 10 years during remeasurement the process of observing disturbance is not always straightforward. For example, in certain situations (mostly involving insects and disease) field crews cannot accurately hind-cast when a disturbance began so instead they label it as "ongoing continuously". In the event of this designation we used the year of plot measurement as a proxy for year of occurrence. Field crews can record up to 3 different disturbances and 3 different treatments (i.e. harvest) for each forested condition found on a plot.

To capture smaller (<4047 m^2) and less severe disturbances (<25% of trees) not captured at the condition-level, we also used FIA's sample tree measurements. This involved calculating the number of individual trees ≥ 12.7 cm (5 inch) DBH on each plot which were flagged as damaged or killed by the same 7 agents used above (e.g. insect, disease, fire, harvest, weather, animal, and other). Trees were summed across all conditions found on the plot. To capture multiple disturbances, all agents with 5 or more impacted trees were recorded as separate disturbance events. Since the timing of tree-level disturbance and mortality is not consistently available when necessary the year of plot measurement was used as a proxy for year of occurrence.

2.2.2. Landsat time series disturbance observations

To derive supplemental disturbance history information for the 449 forested FIA plots we used a new approach for collecting reference information based on human interpretation of remotely sensed data. Similar to the TimeSync methodology (Cohen et al., 2010), we used a trained analyst to manually record disturbance observations based on evidence gleaned from simultaneous inspection of annual Landsat data (both individual images and spectral trajectories), high resolution air photos (e.g. NAIP, Google Earth), and ancillary GIS layers including MTBS fire polygons (Eidenshink et al., 2007) and Landfire disturbance grids (Vogelmann et al., 2011). By concurrently viewing all the available data in and around the plot area, the analyst was able to use the spectral information and supporting context from air photos to record the timing and cause of disturbances occurring on the FIA plots between 1995 and 2011 (see Fig. 2 for example). To minimize spatial inaccuracies in both the image data (e.g. misregistration) and FIA plot locations (e.g. GPS error) we elected to interpret a 4047 m^2 (1 acre) circular area drawn around the center coordinate of each FIA plot. This approximates the area sub-sampled by FIA, which uses 4 sub-plots covering about 1/6 of this area.

Although Landsat data has a 30 m spatial grain, its spectral time series offers a consistent and highly informative signal from which both subtle and abrupt changes in forest structure and leaf area can be resolved (see Fig. 2 lower left, Cohen et al., 2010; Kennedy, Cohen, & Schroeder, 2007; Schroeder, Wulder, Healey, & Moisen, 2012). Here, the Landsat data alone led to the detection of 5 different types of disturbance, including: stress (from insect, disease and drought); fire; harvest; mechanical (e.g. brush saw, chaining); and other (e.g. label used for disturbances which could not be assigned a specific cause). In most cases where disturbance occurred abruptly, the Landsat data could be used to determine the year of onset. The interpretability of the Landsat data was greatly enhanced by the inclusion of higher spatial resolution (~1 m) air photos (e.g. NAIP) such as those commonly found in Google Earth. Covering several dates (1993, 1998, 1999, 2001, 2003, 2004, 2006, 2008, 2009, 2011), the air photos were instrumental in detecting the first signs of stress-related tree mortality caused by insects, disease, and drought. Not surprisingly, the most recent air photos were found to be the best quality (in terms of spatial resolution, color, and contrast) and thus allowed a unique opportunity to improve capture of the recent insect outbreaks which have impacted the study area.

During the analyst interpretation process we observed several instances where widespread, chronic (i.e. slow-developing) tree mortality could be seen in the air photos even though it was not yet distinguishable in the Landsat images or trajectories. Because most of the severe insect damage in this area has occurred within the last 8 years of the study period (i.e. 2004–2011) there were several high quality photos which showed detailed changes in tree-level mortality. Using this improved spatial detail we were able to count the number of red attacked trees (primarily caused by mountain pine beetle) and dead gray trees occurring within each plot's 4047 m^2 (1 acre) footprint (see Fig. 2 lower right). This process involved using the most recent NAIP photo (which was the highest quality) to count the number of disturbed trees in 2011. Then, working backwards, the disturbed trees were pushed back in time as far as possible using the older dates of photography. The year of onset was recorded as the date of the earliest photo containing evidence of tree mortality. Plots observed to have red attack trees were labeled as insect disturbance, whereas plots with only gray dead trees were labeled "stress" to imply mortality may have been the result of any number of slower occurring processes (e.g. insects, disease, or drought). As the spatial detail of this information is similar to FIA's tree-level measurements we considered all plots with 5 or more dead or dying trees as disturbed. We recognize that using the same tree cutoff with larger LTS plots will result in a higher probability of detecting disturbance. As one of the objectives of this study is to improve FIA's sensitivity to detecting disturbance we consider this an advantage of the LTS approach. However, since our estimates are not reported on a per-area basis and do not quantify differing levels of severity (e.g. number of disturbed trees) no adjustment is needed to account for differences in FIA and LTS plot sizes. Note the use of bigger LTS plots will result in larger area estimates than FIA due to the difference in relative numbers of dead trees observed per unit area (e.g. 5 trees per 1/6 acre FIA plot vs. 5 trees per 1 acre LTS plot). Finally, in addition to recording

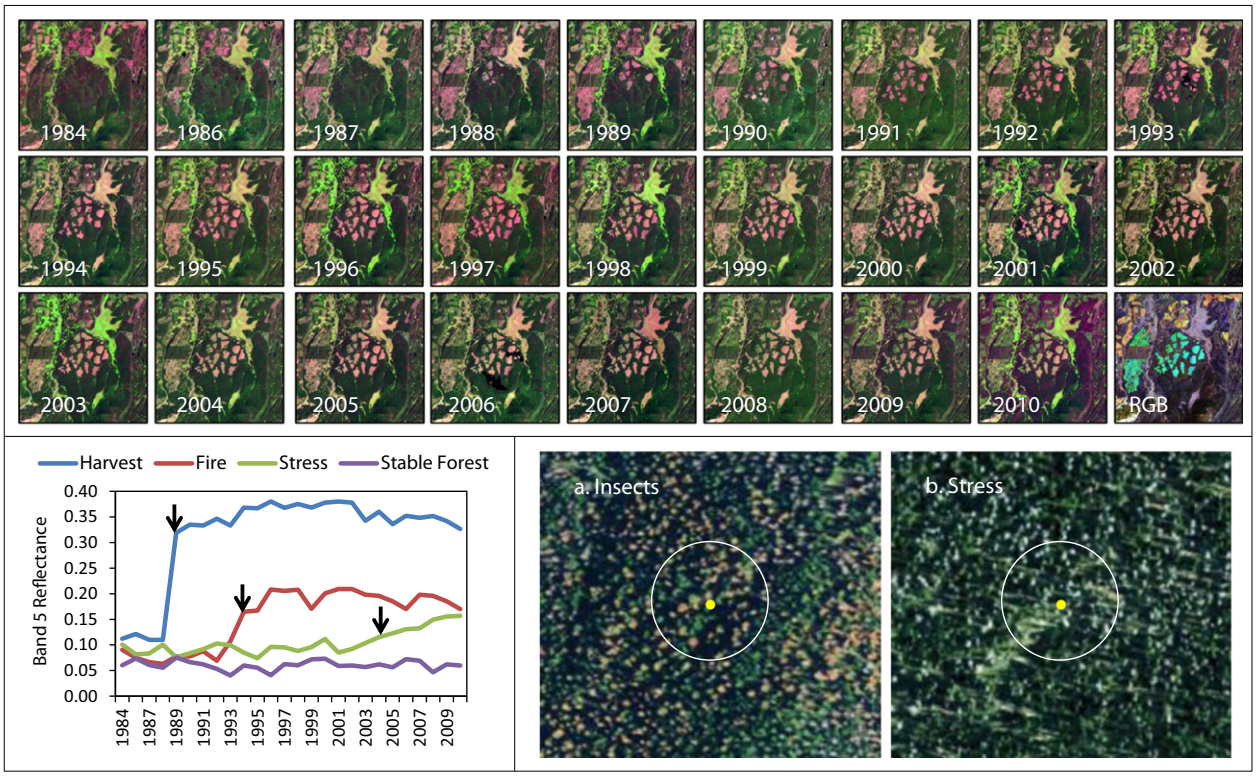

Fig. 2. Example of Landsat time series (LTS) approach used to detect disturbance on FIA plots. Data were displayed so an analyst could simultaneously view the 26 year Landsat time series both as a series of images (top, displayed in 5,4,3 false color; RGB uses band 5 images from 1984, 1999, and 2010) and spectral trajectories (lower left, showing patterns of disturbance with arrows indicating year of onset). A series of high resolution (~1 m) air photos (lower right) were also used to aid the interpretation of the Landsat data, as well as to count the number of trees impacted by a.) insects (e.g. red coloring associated with mountain pine beetle damage) and b.) stress (e.g. disease, drought).

the type and timing of each disturbance (and for insect/stress the number of dead and dying trees) the analyst also estimated the magnitude of each disturbance (i.e. severity) as either very low, low, moderate or high, depending on the amount of observed tree cover change pre- and post-disturbance. Similarly a confidence score was assigned (high, medium, low) which reflected the analysts overall degree of certainty regarding the accuracy of the recorded disturbance attributes. Only disturbances with medium and high confidence were used in the analysis.

2.2.3. Combining FIA and Landsat time series disturbance observations

Given the spatial and temporal complexity of forest disturbance, a hybrid approach which incorporates both FIA and LTS observations may well provide the most complete picture of how disturbance is impacting the broader landscape. Thus, to better understand how the LTS and field observations relate to one another we used the cells of a standard agreement matrix to divide the plots into 3 disturbance populations: 1.) Plots where both LTS and FIA field crews found disturbance (referred to as FIA + LTS), 2.) Plots where only FIA field crews found disturbance (referred to as FIA only), and 3.) Plots where only LTS found disturbance (referred to as LTS only). Here agreement is based solely on the presence of disturbance, thus timing and agent are not explicitly considered. Using these populations, we examine two physical and temporal characteristics of the field and LTS disturbance observations. First, the FIA tree measurements are used to compare the relative canopy position of non-stand clearing disturbances (i.e. insect and stress) detected by FIA and LTS (population 1) versus those found only by FIA (population 2). Cumulative frequency distributions and the non-parametric Mann–Whitney test (reported as U) are used to compare the median size (e.g., HT in m and DBH in cm) of disturbed (i.e. standing dead and disturbed trees ≥ 12.7 cm (5 inch) DBH identified above in Section 2.2.1, plots with only condition-level disturbance and no disturbed trees are not considered) and undisturbed "live" trees ≥ 12.7 cm (5 inch) DBH from the two populations. Note that HT and DBH are first derived as plot-wise averages (without weighting by forested proportion of the plot), which are then summarized and compared as medians across the two populations. No minimum tree cutoff was applied thus all plots with measured tree disturbance were included in the analysis (note trees from the most recent survey were used on remeasured plots). If multiple conditions were observed, the live and dead trees were taken from the same class except in rare cases when availability required using live trees from a secondary condition. In the case where HT and DBH of disturbed trees (excluding fire and harvesting) is larger and significantly different than the undisturbed trees we can infer disturbance occurred in the upper or main stand portion of the canopy; whereas, larger undisturbed trees implies disturbance occurred at, or below main canopy level (i.e. understory). Second, cumulative frequency plots of the number of years between LTS (last measured in 2011) and FIA field measurements are compared to highlight the effect of sampling frequency on disturbance detection. Using all the disturbed plots from the three error matrix populations, a second series of Mann–Whitney tests are used to determine if the LTS only plots have a larger median number of years since FIA's last field visit. A significant discrepancy in the amount of time since last field measurement would indicate that the continuous nature of the LTS observations is an important factor in detecting disturbance between FIA field visits.

2.2.4. Landsat forest disturbance map

In addition to collecting the analyst interpretations, we also used the LTS data to create a forest disturbance map for post-stratification. Due to the widespread and complex nature of the disturbance processes impacting the study area, this required a three step process. First, the near-annual stack of 26 growing season (i.e. one image per year, June

to September) Landsat images (1984–2010) was used to map disturbance with two automated algorithms, the Vegetation Change Tracker (VCT, Huang et al., 2010) and the Landsat-based detection of Trends in Disturbance and Recovery or "LandTrendr" (Kennedy et al., 2010). Even though both algorithms infer change on the ground from changes in the spectral signal captured over time by multiple Landsat images they do so in different ways. For instance, VCT uses an "adaptive thresholding" approach to primarily locate abrupt disturbances such as fire and harvesting, while LandTrendr relies on multitemporal segmentation to simultaneously find both abrupt events and slower, longer-term trends.

Although these algorithms were able to find most of the major disturbances (e.g. fire and harvests) neither was fully optimized to capture the pervasive, low severity damage caused by recent insect outbreaks. Detecting insect disturbance can be challenging for automated algorithms because the spectral changes are usually subtle and slow to develop (Vogelmann, Xian, Homer, & Tolk, 2012) and there is an inherent level of background noise associated with imperfect image calibration, atmospheric correction, and varying sensing geometry. Here the challenge was further exacerbated by the fact the low magnitude changes occurred near the end of the time series and were impacting both dense and sparse forest types. Although LandTrendr and VCT did successfully identify some areas of low magnitude change, the specific needs of our study required a more thorough capture of the recent insect outbreak.

Therefore in a second step, instead of attempting to further customize VCT or LandTrendr, we combined the initial output from those algorithms' with a composite analysis approach (Coppin & Bauer, 1996) using supervised classification of multi-temporal images to target the missed insect damage. The supervised classification, developed with shortwave-infrared data from Landsat band 5, allowed us to better isolate the subtle, yet distinct spectral patterns associated with the insect damage, which in turn led to improved capture of the widespread nature of the disturbance. The third and final step involved using a previously published forest cover map (Blackard et al., 2008) to remove disturbance from non-forest areas. To better coincide with the temporal span of the FIA and LTS observations, only the disturbances mapped between 1995 and 2010 were used in the analysis. Finally, the 30 m resolution map was recoded into three classes (undisturbed forest, forest disturbed between 1995 and 2010, and non-forest) for use in stratifying the design-based estimates of disturbance.

2.3. Design-based estimates of forest disturbance

To derive traditional, design-based estimates of disturbance we used an in-house statistical package called Forest Inventory Estimation for Analysis (FIESTA, Frescino, Patterson, Freeman, & Moisen, 2012). Developed as a flexible estimation tool, FIESTA expands the analytical capacity of traditional FIA state-level reporting to more easily incorporate diverse ancillary layers for reducing estimation variance and for reporting on different areas of interest. Here FIESTA was used to calculate the amount of disturbed area (with 95% confidence intervals) between 1995 and 2011 caused by each of the nine disturbance agents and their total. Note the study period is defined by the range of FIA measurement (starting in 2000 minus a five year look back for disturbance or 1995) and the most recent LTS observations (last measured in 2011). Stratified estimates (developed using the forest disturbance map described above) were calculated with standard estimators outlined in Cochran (1977) and Scott et al. (2005). Due to programming constraints, plots with multiple disturbances were only counted once when estimating total disturbance, thus individual agent estimates will not directly sum to total disturbance. Two estimates were run for each set of disturbance observations (i.e. FIA, LTS, and FIA + LTS), one using the Landsat disturbance map for post-stratification and the other with no stratification (i.e. treated as a simple random sample). To quantify the effectiveness of post-stratification, we converted the standard errors from each run to variance, then calculated relative efficiency (RE) as the ratio of variance from simple random sampling divided by the variance from post-stratification (McRoberts et al., 2006). In general, the higher the RE, the more effective stratification is at increasing the precision of the disturbance estimates. In other words, RE can be thought of as a measure of how much larger a simple random sample would need to be in order to achieve the same level of precision obtained by post-stratification. Any increase in sample size can be further evaluated in terms of potential cost savings to the inventory program.

3. Results

3.1. Comparing FIA field and Landsat time series disturbance observations

Over the 17 year period of study, FIA field crews observed a total of 140 discrete disturbance and treatment (i.e. harvest) events (on 126 out of 449 plots), of which the vast majority (76%) were attributed to insects and disease (Table 1). Fires were the next most prevalent agent (8%), followed by animal (5%), weather (4%), other (3%) and harvest (2%). The types and proportion of disturbances detected on the ground by FIA were similar to those observed by analyst interpretation of the LTS data (Table 1). For example, 84% of the LTS disturbances were attributed to insects and stress, with fires (8%), harvest (4%) and mechanical treatments (3%) the next most prevalent agents. In addition, both the FIA and LTS observations showed that during the period of study, disturbance has been steadily increasing with time (see Fig. 3, note different y-axes). Despite these similarities the LTS approach found 167 disturbance events (on 161 out of 449 plots), nearly 28% more than were recorded by FIA field crews. The importance of the aerial photography was evident as more than half of the LTS disturbances (mostly resulting from insects and stress) were either low or very low severity (Table 2) and thus required the higher spatial resolution photos for detection.

To better understand the physical and temporal dynamics of the LTS and field detected disturbances we compared the plot-level observations using a standard agreement matrix (Table 3). Overall the LTS and FIA field observations agreed 73% of the time, although much of this agreement was attributed to the large number of undisturbed plots (n = 244). When only disturbed plots were considered (n = 205) agreement dropped to 40%. The low kappa statistic (0.37) highlights the large number of disturbances found by only one of methods. In fact, when taken together (n = 123) the unique detections account for 60% of all plot-level disturbances. The error matrix was used to divide the plots into three populations which were used to further analyze two physical and temporal characteristics of the LTS and field detected disturbances.

First, to assess the relative canopy position of the detected disturbances we compared distributions of disturbed and undisturbed tree size (e.g. HT and DBH from FIA measurements) using plots from populations 1 (FIA + LTS) and 2 (FIA only). Table 4 shows that when LTS and FIA crews both found disturbance (population 1) the disturbed

Table 1
Types and frequency of disturbance observed by FIA field crews and Landsat time series (LTS) interpretation (n = 449 plots).

	FIA	LTS	FIA + LTS
Insect	58	93	108
Disease	49	0	49
Stress	0	47	21
Fire	11	14	15
Harvest	4	7	10
Weather	6	0	6
Mechanical	0	5	5
Animal	7	0	7
Other	5	1	3
Total # of disturbance events	140	167	224
Total # of disturbed plots	126	161	205

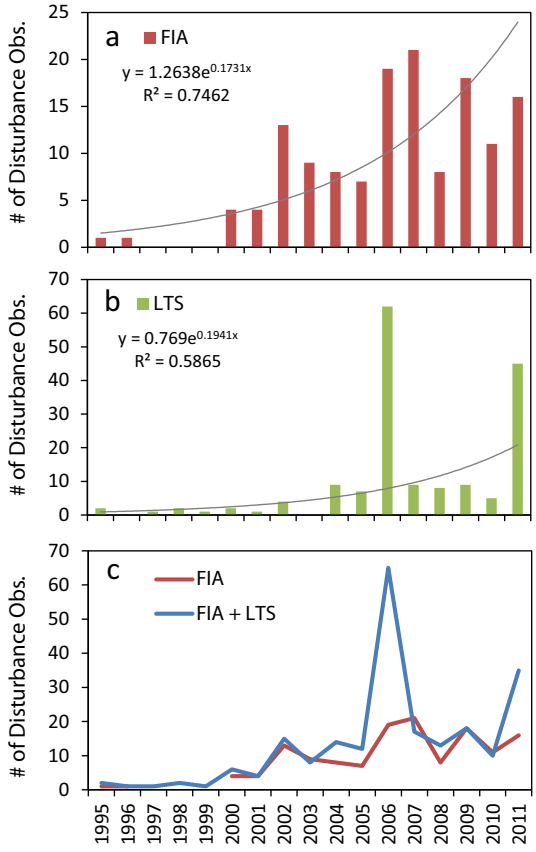

Fig. 3. Temporal frequency of disturbance events observed by a.) FIA field crews (FIA), b.) analyst-led Landsat time series (LTS) interpretation, and c.) a combination of FIA and LTS data (FIA + LTS); note different y-axes. In a. and b. fitted exponential curves (gray lines) show disturbance has been increasing in the Uinta Mountains over the 17 year period of study.

trees were significantly taller (median HT DISTURB = 14.48 m, U = 1721, p = 0.010) and larger (median DBH DISTURB = 23.37 cm, U = 1741, p = 0.013) than the undisturbed "live" trees (median HT LIVE = 13.05 m, median DBH LIVE = 21.41 cm). On the other hand, plots with only FIA disturbance (population 2) showed no statistical difference in the size of disturbed and undisturbed trees (HT LIVE vs. HT DISTURB U = 351, p = 0.815 and DBH LIVE vs. DBH DISTURB U = 299, p = 0.257). Cumulative frequency distributions of HT and DBH (Fig. 4) further highlight the size difference between disturbed and undisturbed trees for population 1 (FIA + LTS, top row) versus no difference for population 2 (FIA only, bottom row).

A second series of Mann–Whitney tests were run to gauge the effect of sampling frequency on disturbance detection. This involved using the three error matrix populations to compare the median number of years between LTS observation (last measured in 2011) and FIA field measurement. Table 5 shows that the LTS only plots (population 3) had a significantly larger median number of years since last FIA field measurement (6 years) than either of the other two populations

Table 2
Number of Landsat time series (LTS) disturbance observations by severity class.

	High	Moderate	Low	Very low	Total
Insect	27	17	24	25	93
Stress	6	7	19	15	47
Fire	5	8	1	–	14
Harvest	2	3	2	–	7
Mechanical	2	1	1	1	5
Other	–	–	1	–	1
Total	42	36	48	41	167

Table 3
Matrix showing plot-level agreement between FIA field crew and Landsat time series (LTS) disturbance observations. Here agreement is based solely on the presence of disturbance without explicit consideration for onset year or agent type. Numbered cells (shown in bold) refer to the 3 disturbance populations used in the distribution analyses presented in Tables 4 and 5 and Figs. 4 and 5.

	Landsat time series obs.			
FIA field obs.	Disturb	Not Disturb	Total	Commission
Disturb	**1** 82	**2** 44	126	34.92%
Not disturb	**3** 79	244	323	24.46%
Total	161	288	449	
Omission	49.07%	15.28%		
Overall agreement = 0.73; Kappa = 0.37				

(FIA + LTS = 2.5 years, U = 1582, p = 0.000 and FIA only = 2.0 years, U = 871, p = 0.000). Essentially, LTS is catching a significant amount of disturbance on plots for which the last field measurement was several years ago. The magnitude of this difference is further highlighted by the cumulative frequency plot (Fig. 5) which shows that 50% of the population 1 and 2 disturbances occurred within 3 years (or less) of the most recent LTS measurement, while 50% of the LTS only disturbances (population 3) occurred on plots which were last visited by FIA 6–9 years ago.

3.2. Landsat forest disturbance map

In an attempt to improve the precision of the design-based estimates a Landsat disturbance map was developed for post-stratification. The multi-step process used to develop the map is described in Fig. 6 (panels a–f). First, VCT and LandTrendr were run over the study area resulting in a disturbance map which captured abrupt, large magnitude changes from fire and harvesting, as well as some areas of low magnitude insect damage (Fig. 6a and d). The output from VCT and LandTrendr was then combined with a supervised classification which used unique shortwave-infrared (band 5) training signatures (Fig. 6f) and a maximum likelihood classifier to specifically target the insect damage missed by the automated algorithms (Fig. 6b and e). A close up (Fig. 6 panels c–e) shows how the majority of forest along the north slope of the Uinta range has spectrally changed from a healthy, green color in 1987 to a stressed, dark purple color in 2010 (images are displayed in 5,4,3 false color). Combining the outputs from the supervised and automated approaches dramatically improved the capture of the pervasive insect damage (Fig. 6e). From a simple disturbed versus not disturbed perspective (i.e. timing and agent are not considered) this "combined" disturbance map agreed well (e.g. overall agreement = 75.5%, +/−2.1%) with the LTS disturbance observations described above in Section 2.2.2.

Table 4
Mann–Whitney U results comparing FIA measurements of height (HT) and diameter at breast height (DBH) of disturbed and undisturbed trees for populations 1 (FIA + LTS, n = 68) and 2 (FIA only, n = 27) of the agreement matrix shown in Table 3. Populations with statistically different medians are highlighted in bold. Note only non-stand clearing disturbances are considered.

Population 1 – FIA + LTS (n = 68)	Median	U	p-Value
HT LIVE (m)	**13.05**	**1721**	**0.010**
HT DISTURB (m)	**14.48**		
DBH LIVE (cm)	**21.41**	**1741**	**0.013**
DBH DISTURB (cm)	**23.37**		
Population 2 – FIA only (n = 27)	Median	U	p-value
HT LIVE (m)	11.69	351	0.815
HT DISTURB (m)	12.13		
DBH LIVE (cm)	22.81	299	0.257
DBH DISTURB (cm)	21.08		

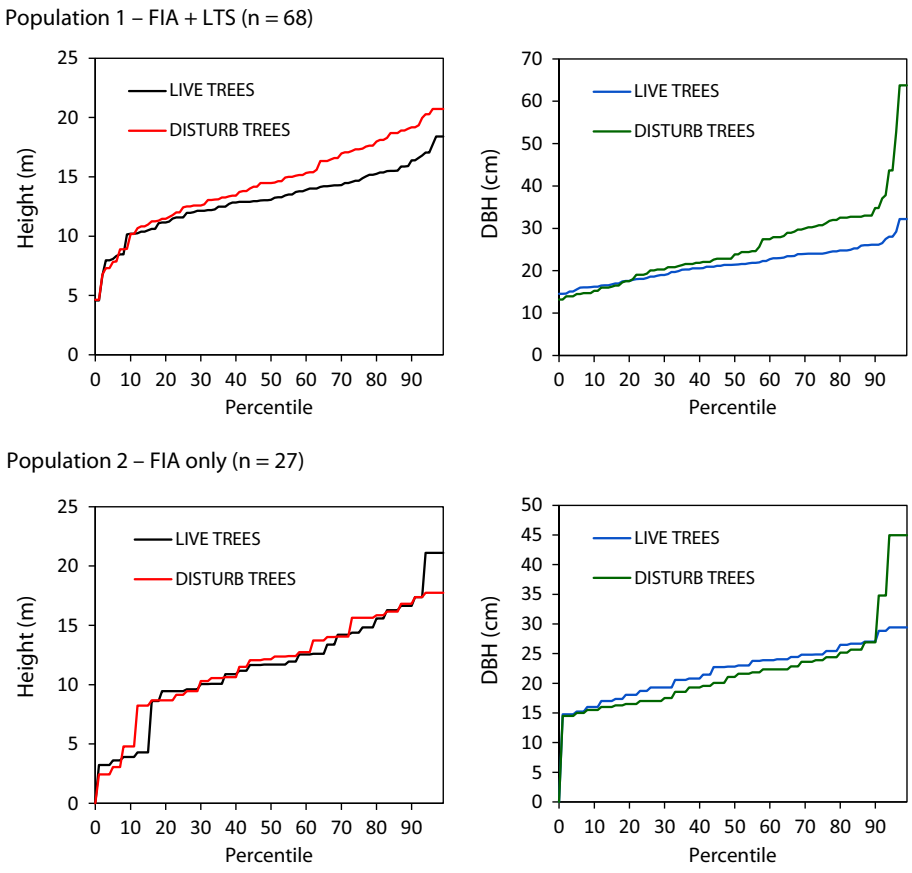

Fig. 4. Cumulative frequency distributions showing FIA measurements of height (HT) and diameter at breast height (DBH) of disturbed (red and green lines) and undisturbed (black and blue lines) trees for populations 1 (FIA + LTS, top row, n = 68) and 2 (FIA only, bottom row, n = 27) of the agreement matrix shown in Table 3. Note only non-stand clearing disturbances are considered.

3.3. Design-based forest disturbance estimates

Estimates of the amount of disturbed forest occurring between 1995 and 2011 were generated for the Uinta Mountains study area using observations from FIA field crews, analyst-based LTS interpretation and a combination of FIA and LTS data. Although the estimates were run with and without the Landsat map for post-stratification, only the post-stratified estimates are shown for brevity (the effectiveness of post-stratification is evaluated below). The amount of forest disturbed (in ha with 95% confidence intervals) by each of the nine disturbance agents is shown in Fig. 7a and b. The agents which occurred less frequently (shown in Fig. 7a) have large confidence intervals relative to area disturbed due in part to high sampling errors resulting from low sample size. Several of these agents were only observed by one method (e.g. weather, mechanical, and animal) while others (e.g. fire and harvest) have FIA estimates that are well below (25% and 40% less respectively) those from LTS. The FIA + LTS observations resulted in the largest estimates of fire (33,177 ha) and harvest (24,352 ha), indicating that each method found unique events that were not detected by the other. Furthermore, the FIA + LTS observations also led to improved agent labeling. For example, estimates of other disturbance were much higher for FIA (12,833 ha) than LTS (2344 ha); however, when the data were combined, more than half of FIA's "other" disturbances were also observed by LTS, and thus could be reassigned to more specific agent classes. This same data combining effect also allowed nearly 50% of the LTS stress to be reassigned to more descriptive insect and disease categories (Fig. 7b). Insects were by far the most prevalent agent with FIA + LTS combining to estimate 259,496 ha (+/−40,791) of disturbance.

Table 5
Mann–Whitney U results comparing number of years between LTS (last measured in 2011) and FIA field measurements for the three agreement matrix populations shown in Table 3. Populations with statistically different medians are highlighted in bold.

	n	Median (years)	U	p-Value
Population 1 — FIA + LTS	82	2.5	1764	0.836
Population 2 — FIA only	44	2.0		
Population 1 — FIA + LTS	**82**	**2.5**	**1582**	**0.000**
Population 3 — RS only	**79**	**6.0**		
Population 2 — FIA only	**44**	**2.0**	**871**	**0.000**
Population 3 — RS only	**79**	**6.0**		

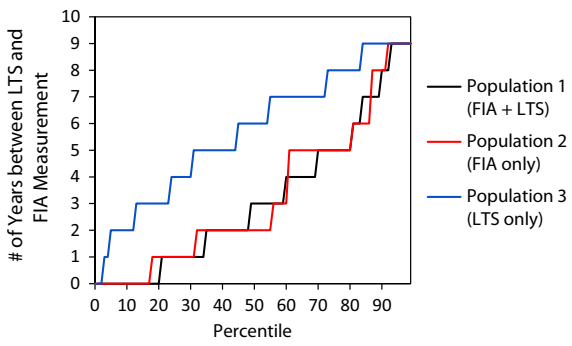

Fig. 5. Cumulative frequency distributions showing number of years between LTS (last measured in 2011) and FIA field measurements for the three agreement matrix populations shown in Table 3.

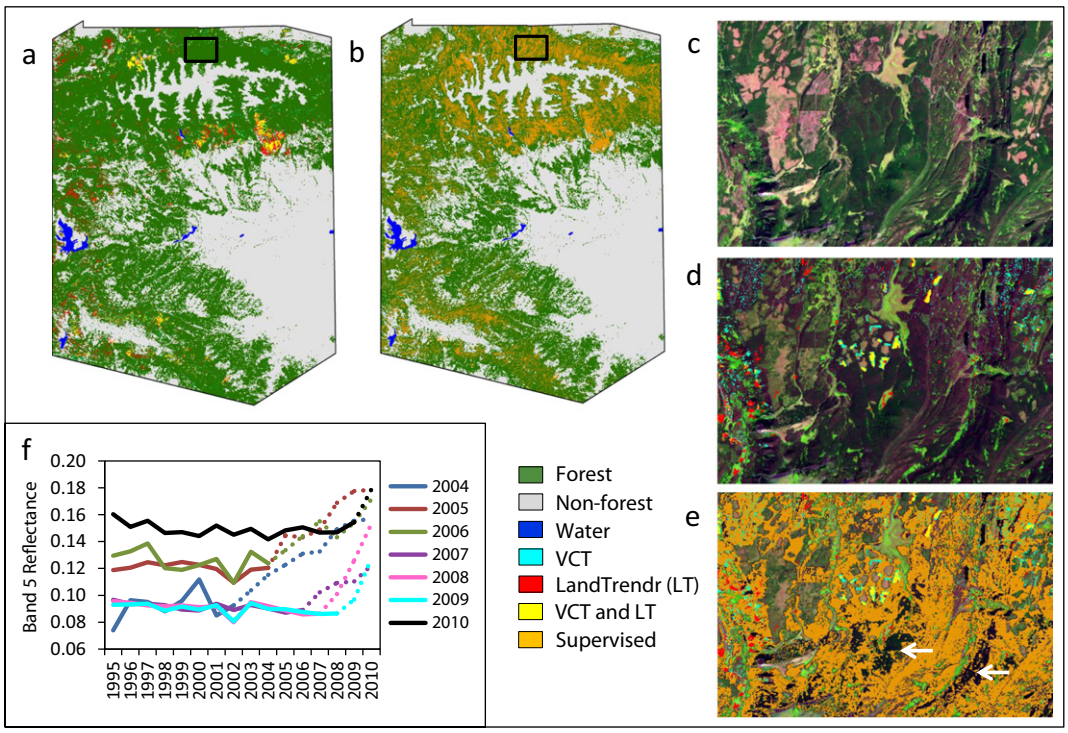

Fig. 6. A forest disturbance map was created for the study area by combining output from a.) VCT and LandTrendr (LT) with b.) a supervised classification of insect and stress damage. A close up view (panels c–d) highlights how the forest has undergone a noticeable spectral change from c.) a healthy dark green color in 1987 to d.) a stressed, dark purple in 2010 (images are displayed in 5,4,3 false color). Panel d shows that VCT (cyan) and LT (red) capture abrupt disturbances (i.e. fire, harvest) but omit stress and insect damage (purple). Panel e shows how combining VCT and LT with the supervised classification improves capture of the full scope of the disturbance. White arrows in panel e highlight areas of disturbance which were missed due to topographic shadowing. The shortwave-infrared training signatures used to classify the stress and insect damage are shown in panel f (dotted lines approximate the year of onset).

When taken across agents, estimates of total disturbance (Fig. 8) had proportionally smaller, non-overlapping confidence intervals. The FIA field data yielded the lowest estimate of total disturbance (294,295 ha, +/−44,242) followed by the LTS estimate which was 32% higher (389,151 ha, +/−44,849). The FIA + LTS observations led to the largest estimate which found 486,458 ha (+/−47,101) of forest was disturbed during the 17-year period of study. Overall the combined estimate is 65% higher than the estimate derived solely with the FIA field data.

The effectiveness of using the Landsat disturbance map for post-stratification was assessed using the measure of relative efficiency (RE). The REs for each agent class and for total disturbance are presented in Table 6. In general, estimates derived with the LTS response data benefited more from post-stratification than estimates derived solely with the FIA field data. Most of the individual agents saw very little if any benefit from stratification although some of the more prevalent agents like insects (RE = 1.26) and fire (RE = 1.16) did show some minimal improvement. Because the disturbance map did not specifically label causal agents, it is not surprising that the estimates of total disturbance gained the most benefit from post-stratification. Total disturbance estimates derived with the LTS and combined FIA + LTS data saw the biggest gains in precision with REs of 1.43 and 1.50 respectively. According to the 5 levels of gain outlined by Czaplewski and Patterson (2003), REs of this magnitude represent moderate improvement such that the simple random sample of forested FIA plots would need to increase by 43–50% to achieve the same level of precision obtained by post-stratification.

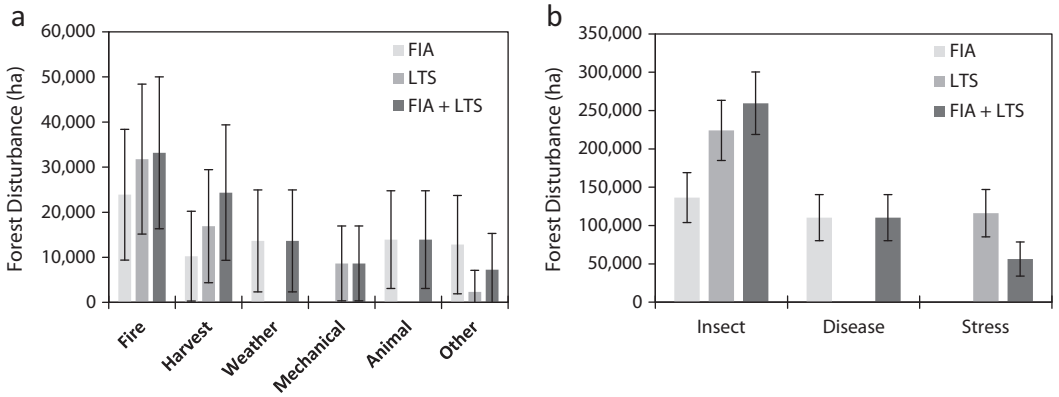

Fig. 7. Forest disturbance estimates with 95% confidence intervals based on FIA field data (FIA), analyst-led Landsat time series (LTS) interpretation, and a combination of FIA and LTS data (FIA + LTS). The estimates represent the number of hectares (ha) disturbed between 1995 and 2011 for a.) less frequently occurring agents and b.) more prevalent agents such as insects, disease and stress.

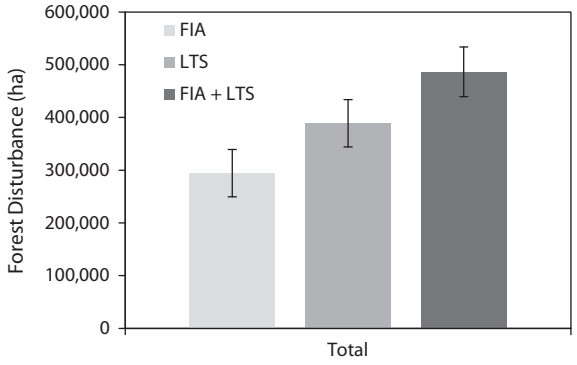

Fig. 8. Estimates of total forest disturbance (in hectares, ha) between 1995 and 2011 with 95% confidence intervals based on FIA field data (FIA), analyst-led Landsat time series (LTS) interpretation, and a combination of FIA and LTS data (FIA + LTS).

4. Discussion

4.1. Disturbance observations

In this study, a new LTS methodology was used to integrate various scales of data to improve estimates of disturbance from a design-based sample of FIA plots located in the Uinta Mountains of Utah, USA. This involved using an analyst to record forest disturbances based on visual evidence gathered from annual Landsat images, NAIP photography, and other ancillary spatial data sets (e.g. MTBS, Landfire) (Fig. 2). One advantage to this approach is that it allows all plots to be measured annually with remote sensing data, resulting in improved temporal sensitivity compared to the FIA sample design, which requires 10 full years to visit all of the plots in this study area. In addition, the LTS approach was adapted to take full advantage of high resolution photography, which allowed tree level mortality caused by insects to be captured on each plot (Fig. 2, lower right). The high spatial resolution of these observations (~1 m) coupled with the larger, 4047 m^2 (1 acre) LTS plot size improved detection of low severity disturbance involving only a few trees and thus helped bridge the spatial gap between the Landsat images (30 m pixel) and the FIA field observations.

Overall, the improved spatial and temporal sampling of the LTS approach led to the detection of 28% more discrete disturbance events than were recorded solely by FIA crews (Table 1). Much of the increase in detection is attributed to the more current and continuous observations provided by the LTS measurements (see Table 5 and Fig. 5), though the use of bigger measurement plots was also a contributing factor. Although LTS detected more disturbance, the FIA field observations were critical for capturing below-canopy processes (see Fig. 4 bottom row) which were not detectable from the aerial perspective (e.g. animal damage, weather and ground fires) and for providing better labeling of disturbances caused by insects and disease (Table 1). Although combining the observations improves capture we recognize that some below-canopy disturbances may still be missed due to our temporal updating approach relying solely on imagery and photos that look down on top of the canopy.

Despite differences in viewing perspective and sampling frequency, both the LTS and FIA observations show that disturbance in the Uinta Mountains has been increasing with time (see fitted exponential curves Fig. 3). This increase is due in large part to widespread insect outbreaks (mostly from mountain pine beetle) which started around 2004. Although both observation methods show a distinct increase in disturbance around this time, the LTS data show two pronounced peaks in 2006 and 2011. These peaks are largely caused by the spacing, quality and availability of the air photos which were the primary data used to detect most of the LTS insect and stress disturbance. Though the photos do not always support an accurate assignment of onset year, they do provide improved capture of the overall impacts of disturbance across the study period. In general, the availability and quality of data, coupled with the timing and natural characteristics of the disturbance agents at play in a particular region, will impact the exact implementation of the analyst interpretation methodology as presented in this study. As data quality and availability are generally improving with time (Wulder, Masek, Cohen, Loveland, & Woodcock, 2012), it seems likely that some variant of the presented approach could be implemented in most areas of the country (Loveland & Dwyer, 2012).

In this study more than half of all plot-level disturbances were detected with only one of the two observation methods (FIA only n = 44; LTS only = 79), thus strongly supporting our case for using a plurality of evidence to maximize disturbance detection. Using the FIA tree measurements we established that FIA crews add below canopy disturbances (Fig. 4, bottom row; Table 4, population 2), while LTS adds disturbance primarily through improved temporal sampling (Fig. 5, Table 5). These findings are clearly related to the scale of observations, with field crews able to access individual-tree disturbance information and LTS picking up disturbance occurring both between sub-plot measurements and since the time of the last field survey. Our results suggest that combining the LTS and FIA field methods may improve the acuity with which an inventory picks up disturbance. Additionally, if it is determined that a particular disturbance processes is being missed by an inventory, the integrative approach presented herein opens the door for specialized LTS analyses in addition to altering existing field protocols. These benefits extend to other probabilistic sets of field inventory measurements and are thus not restricted to FIA.

Although some upper canopy, non-stand clearing disturbances were detected from the field and aerial perspectives (Fig. 4 top row, Table 4 population 1); the conditions were such that only a small percentage of total disturbance was detected by both methods (see Table 3, population 1). Partial disturbance may be detected and characterized with LTS (e.g. Healey, Yang, Cohen, & Pierce, 2006; Kennedy et al., 2010), but spectral signals are more subtle than those associated with stand-clearing events, and are thus more difficult to isolate in the context of normal phenological and radiometric variation. At the same time, many types of partial disturbance do not alter a field list of live trees; such disturbances may significantly alter a stand's canopy (branches and/or foliage) without causing mortality and the loss of individual stems. Given these potential barriers to detection of partial disturbances, it is unsurprising that there was relatively little overlap in detection between the field and remotely sensed methods.

One issue not addressed in our estimates, nor in those of FIA, is the error associated with observing disturbance. Photo interpretation error will certainly affect the quality of the LTS estimates, and field measurement error also exists. FIA disturbance measurements generally meet program quality standards; however this is largely because disturbance tends to be rarely observed (Pollard et al., 2006). Agreement between "cold check" field calls can be poor in cases where at least one crew observes a disturbance. Though this work was restricted to FIA's standard design-based estimators, other methods may be more appropriate for

Table 6
The relative efficiency (RE) of using the Landsat disturbance map to post-stratify the design-based estimates shown in Figs. 7 and 8 (FIA = Field, LTS = Landsat time series). The higher the RE the more effective stratification was at improving the estimate over simple random sampling.

	FIA	LTS	FIA + LTS
Insect	1.11	1.20	1.26
Disease	1.01	–	1.01
Stress	–	1.02	0.99
Fire	1.10	1.16	1.15
Harvest	0.97	0.99	1.00
Weather	0.96	–	0.96
Mechanical	–	1.00	1.00
Animal	0.94	–	0.94
Other	0.93	1.07	0.95
Total	1.15	1.43	1.50

variables such as disturbed area (e.g., McRoberts & Walters, 2012), and are thus an area of future research.

4.2. Landsat forest disturbance map

To examine benefits of post-stratifying the plot-based estimates, a Landsat disturbance map was produced for the study area. With several different types of disturbance agents at play, a multi-step process was required to capture the varying levels of damage found across the region. Here the automated algorithms VCT and LandTrendr provided a quick and reliable way of mapping abrupt, severe disturbances (e.g. fire and harvesting); however in this study neither was fully optimized to capture the slower, pervasive damage caused by recent insect outbreaks. We recognize that specialized calibration efforts with these algorithms, particularly LandTrendr (Kennedy et al., 2010) would likely have resulted in better capture of insect activity. There are also other recent approaches to LTS analysis (Brooks, Wynne, Thomas, Blinn, & Coulston, 2014; Zhu et al., 2012) which leverage a very high density of historic Landsat observations to detect even slight deviations from established conditions. Since several factors complicate remote detection of insect disturbance (e.g. forest condition and age structure, type and intensity of pest activity, and timing, repeatability and resolution of input image data), and knowing that the post-stratification role intended for the maps is sensitive to map accuracy (Czaplewski & Patterson, 2003), we opted to use a simple classification approach rather than attempt further calibration of the automated algorithms. The option chosen involved using a detailed set of shortwave-infrared (band 5) training signatures (shown in Fig. 6f) to specifically target the insect damage missed by the automated algorithms. Fig. 6e clearly shows that combining the automated and supervised classifications improved capture of the widespread impacts of the recent insect outbreak.

Though improved, the combined map still contained some large patches of insect damage which were omitted from the classification (see white arrows Fig. 6e). Closer inspection revealed many of these areas were located in dense, mature conifer stands containing very low levels of tree mortality. As mature conifer is spectrally dark in the shortwave-infrared region, it's likely that low levels of tree mortality were masked by shadows (from canopy and topography) and thus did not trigger a large enough spectral response to be classified as disturbance. Our extensive work in this area suggests that spectral indices which respond more directly to changes in leaf area (e.g. NDVI, NBR) may be better suited to distinguishing subtle, low severity changes (mostly related to brightness) occurring in dense conifer forests.

Despite omitting some areas of low magnitude insect damage, our two-stage mapping approach did produce a suitably accurate forest disturbance map for the study area. When compared with the LTS disturbance observations described in Section 2.2.2 above, the map had relatively low error rates for the disturbed forest class (i.e. 48.8% +/− 7.9 omission and 28.3% +/− 8.5 commission). As the map was designed primarily for post-stratification, the low error rate for the disturbance class facilitated effective post-stratification of the sample. Overall, the success of the mapping approach hinged on combining data from multiple algorithms to best capture disturbance. Although VCT and LandTrendr did not capture the full extent of the insect and stress damage, ongoing developments suggest that in the future these algorithms will more successfully capture these trends, thus decreasing (or eliminating) the need to employ labor intensive, post-classification approaches such as the one presented in this study. However, given the complex ecological and spectral dynamics associated with forest disturbance (especially insects e.g. see Meigs, Kennedy, & Cohen, 2011) it is unlikely that any one algorithm will fully capture its distribution on the landscape. In fact, detecting different disturbance patterns around the globe will likely require a variety of different LTS transformations (Schroeder et al., 2012), search algorithms and frequencies of image acquisition (Kennedy et al., 2014). Here, we simply added maps from different algorithms; however this is just a precursor to more sophisticated methods which can statistically integrate maps (from many different algorithms) and other spatial predictors in an ensemble modeling framework.

4.3. Design-based forest disturbance estimates

Estimated amounts of forest disturbance were ultimately determined by the number of discrete disturbance events observed by FIA field crews and/or LTS interpretation. As both methods found unique events not found by the other each resulted in very different estimates of disturbance. For example, Fig. 8 shows that the FIA, LTS and combined FIA + LTS estimates are unique in that none of their 95% confidence intervals overlap each other. At the agent class level, a similar but slightly less unique pattern of estimates was observed for abundant classes like insect and stress (Fig. 7b), whereas rarer classes (with higher sampling error) had larger uncertainty bounds which resulted in different but mostly overlapping estimates of disturbance (Fig. 7a). When examining the estimates it is particularly important to note the large difference between the FIA and FIA + LTS approaches. This difference (nearly 193,000 ha) is considerable especially when viewed as a percentage of total forest area (1,092,046 ha, +/− 42,808). For example, the FIA data suggests that 27% of the total forest area was disturbed during the 17-year period of study as opposed to nearly 45% when FIA + LTS data are combined and used together. Overall, the combined data yields nearly 1.65 times more disturbance over the period of study or nearly 1% more on an annual basis. This dramatic difference further highlights the advantage of augmenting infrequent, but detailed field inventory observations (from FIA and/or other probabilistically collected field plots) with frequent, LTS observations that more robustly sample the full landscape over space and time. While LTS added disturbance through improved temporal sampling (see Table 5 and Fig. 5) the use of larger plots also helped increase detection sensitivity. The large number of unique disturbances observed only by FIA field crews ($n = 44$) and LTS interpretation ($n = 79$) provide strong evidence that combining data from the two approaches leads to a more spatially and temporally complete estimate of disturbance.

In addition to combining the field and LTS observations, the disturbance estimates were further improved by using the Landsat disturbance map for post-stratification. Although derived independently, the success of the stratification as measured by RE (Table 6) showed a clear relationship between the aerial perspective used to collect the disturbance observations and the Landsat perspective used to derive the disturbance map. Post-stratification reduces estimate variance only if plots are effectively grouped into strata with comparatively lower internal variance. To the extent that photo- and satellite-based observations have the same downward-looking perspective of the canopy, it is logical to expect satellite-based maps to correspond to observations made with photos. Those disturbances detectable only from the ground perspective are less likely to be effectively stratified using Landsat-based maps, as our results show (see Table 6). Consequently, lowering sample error by increasing field visits (either by increasing measurement frequency or adding new plots) may be the best way to improve precision of below canopy disturbance estimates. Alternatively, repeated acquisition of canopy penetrating LiDAR may also provide future opportunities for detecting loss of subcanopy trees.

Because specific agent class maps were not available at the time of this study we elected to use a simplistic coding scheme to test broad strata classes developed from a binary disturbance map (i.e. disturbed, undisturbed). Undoubtedly, this limited our ability to effectively stratify most of the individual agent classes; especially those with lower prevalence (e.g. see animal and weather Table 6). In the future, new maps which are currently under development will employ more sophisticated methods to spatially predict individual agent classes, thus potentially allowing improved stratification of specific types of disturbance. To further support management objectives, future studies will also seek

to quantify different severity levels (e.g. Table 2), as well as year to year trends over time (e.g. Fig. 3).

Future improvements notwithstanding, the simple stratification approach used here did result in significant improvement of the LTS and combined FIA + LTS estimates of total disturbance. Based on the REs in Table 6, the FIA simple random sample of forested plots would need to increase by 43–50% to achieve the same level of precision obtained by post-stratification. It must be emphasized that RE here is evaluated not against current FIA estimates (which rely on a variety of point-in-time condition maps around the country), but against a more generally interpretable no-stratification scenario. The RE values in Table 6 are low compared to static variables such as forest area and volume (which have resulted in REs ranging from 2.0 to 5.0 see Gormanson et al., 2003; McRoberts et al., 2006). However, they are on the upper end of studies attempting to stratify dynamic variables such as growth, mortality, and removal (see Brooks et al., 2013). Here increasing the forest sample by 50% would require adding roughly 230 extra field plots to the FIA sample. Assuming a cost of $1000/plot the use of the Landsat disturbance map for post-stratification in this small study area (~1.6 million ha) could net well over $230,000 in potential cost savings over a 10 year cycle. Without question, more accurate disturbance maps which include specific agent classes and more homogenously defined strata classes could in the future lead to even bigger financial savings.

One final issue which impacted map accuracy and ultimately the success of post-stratification is how the inventory plots were assigned to map strata classes. In the presented example, FIESTA used the Landsat pixel from the center of each FIA plot to assign one of the three strata classes (i.e. undisturbed forest, disturbed forest, and non-forest). The use of only one 30 m pixel however meant that a large proportion (>70%) of each plot was not considered when assigning the strata classes. In areas like the Uinta Mountains which experience high levels of spatially heterogeneous disturbance (e.g. insects and disease), this spatial disconnect between the map area unit and the reference sample unit can reduce map accuracy and change the balance of omission and commission errors (McRoberts et al., 2005). This has important implications as both the accuracy and consistency of misclassification impact the success of post-stratification (Czaplewski & Patterson, 2003). As other studies have shown the benefit of modeling FIA plot variables with a 3 × 3 (90 × 90 m) window (Healey, Lapoint, Moisen, & Powell, 2011), there is some justification for incorporating information from surrounding pixels into future strata map assignment procedures. Filtering may be one way to aggregate information and improve performance (Nelson, McRoberts, Holden, & Bauer, 2009) and thus will be a focus of future investigations.

5. Conclusion

In this study we demonstrate two ways LTS can improve traditional, design-based forest inventory estimates of disturbance derived from FIA data. First, a 26 year satellite time series was used to collect supplemental disturbance history information on 449 forested FIA plots located in the central Uinta Mountains of Utah, USA. This involved using a trained analyst to interpret and record the cause and timing of all disturbances occurring on each FIA plot between 1995 and 2011. As the study area has recently experienced high levels of widespread, low severity tree mortality (e.g. insects and disease) the analyst also used a periodic time series of high resolution air photos (e.g. NAIP and Google Earth) to estimate the number of disturbed (i.e. dead and actively dying) trees on each plot. Comparing the plot-level observations, we found FIA and LTS disturbance agreed only 40% of the time, while 60% of disturbances were unique to one method. Using the FIA tree measurements we showed that FIA crews add below-canopy disturbance while LTS interpretation adds disturbance primarily through improved temporal sampling. Here the LTS interpretation approach allowed all FIA plots to be updated annually, a substantial improvement over the 10 year re-measurement cycle typically employed by FIA in the western U.S. Further, by incorporating the improved spatial detail of the air photos, the LTS approach helped bridge the gap between the Landsat and FIA scales of measurement, leading to the detection of 28% more disturbance events than were recorded solely by FIA field crews. Not surprisingly, when the FIA and LTS observations were combined the resulting estimate of total disturbance was 1.65 times higher than the estimate based solely on FIA data. In addition to augmenting the FIA response design, we also used the LTS data to develop a Landsat forest disturbance map for post-stratification.

To improve capture of subtle, yet widespread insect damage, we used a mapping process which combined outputs from automated and supervised classification approaches. Using the measure of relative efficiency (RE), we found post-stratification mostly improved estimates derived with the LTS response data. In fact, the LTS and combined FIA + LTS estimates of total disturbance gained moderate levels of efficiency (REs equal to 1.43 and 1.50, respectively) such that the sample of forested FIA plots would need to increase by 43–50% to attain the same levels of precision achieved by post-stratification. Overall, the improved spatial (i.e. bigger plots) and temporal (i.e. annual measurement) sampling permitted by the LTS approach, coupled with the detailed labeling of below-canopy disturbances observed during FIA field visits, helped formulate the largest and most accurate estimate of disturbance for the study area. Furthermore, post-stratification with the disturbance map helped reduce variance, thus providing an additional way LTS improved the inventory estimates of disturbance. We believe the methodology and results presented in this study outline a novel yet achievable way to improve both plot and landscape level monitoring and estimation of disturbance with FIA plot data. Overall, our results offer a promising look at how LTS observations (both from maps and analyst interpretation) can be combined with FIA and/or other probabilistic sets of field inventory plots to improve estimates of disturbance.

Acknowledgments

This research was funded by the National Aeronautics and Space Administration (NASA) Terrestrial Ecology Program through the North American Forest Dynamics (Phase 3) project. Additional support was provided by the Interior West Region of the US Forest Service's Forest Inventory and Analysis (FIA) program, FIA's Techniques Research Band (TRB), and NASA's Applied Science Program. Additional technical assistance was provided by the US Forest Service's Remote Sensing Application Center (RSAC) and the Laboratory for Applications of Remote Sensing in Ecology (LARSE) part of the U.S. Forest Service's PNW Research Station and Oregon State University.

References

Asner, G. P. (2013). Geography of forest disturbance. *Proceedings of the National Academy of Sciences, 110*(10), 3711–3712.

Bentz, B. J., Régnière, J., Fettig, C. J., Hansen, M. E., Hayes, J. L., Hicke, J. A., et al. (2010). Climate change and bark beetles of the western United States and Canada: Direct and indirect effects. *BioScience, 60*(8), 602–613.

Blackard, J., Finco, M., Helmer, E., Holden, G., Hopppus, M., Jacobs, D., et al. (2008). Mapping U.S. forest biomass using nationwide forest inventory data and moderate resolution information. *Remote Sensing of Environment, 112*, 1658–1677.

Bradford, J. B., Jensen, N. R., Domke, G. M., & D'Amato, A. W. (2013). Potential increases in natural disturbance rates could offset forest management impacts on ecosystem carbon stocks. *Forest Ecology and Management, 308*, 178–187.

Brooks, E. B., Coulston, J. W., Wynne, R. H., & Thomas, V. A. (2013). Improving the precision of dynamic forest parameter estimates using Landsat. (E.B. Brooks Ph.D. Dissertation). *Fourier series applications in multitemporal remote sensing analysis using Landsat data* (pp. 85–112). Blacksburg, VT: Virginia Polytechnic Institute and State University.

Brooks, E. B., Wynne, R. H., Thomas, V. A., Blinn, C. E., & Coulston, J. W. (2014). On-the-fly massively multitemporal change detection using statistical quality control charts and Landsat data. *IEEE Transactions on Geoscience and Remote Sensing, 52*, 3316–3332.

Cochran, W. G. (1977). *Sampling techniques* (3rd ed.). New York, NY: John Wiley & Sons (428 pp.).

Cohen, W. B., & Goward, S. N. (2004). Landsat's role in ecological applications of remote sensing. *BioScience, 54*(6), 535–545.

Cohen, W. B., Yang, Z., & Kennedy, R. E. (2010). Detecting trends in forest disturbance and recovery using yearly Landsat time series: 2. TimeSync — Tools for calibration and validation. *Remote Sensing of Environment*, *114*, 2911–2924.
Coppin, P. R., & Bauer, M. E. (1996). Digital change detection in forest ecosystems with remote sensing imagery. *Remote Sensing Reviews*, *13*, 207–234.
Czaplewski, R. L., & Patterson, P. L. (2003). Classification accuracy for stratification with remotely sensed data. *Forest Science*, *49*(3), 402–408.
Dale, V. H., Joyce, L. A., McNulty, S., Neilson, R. P., Ayres, M. P., Flannigan, M.D., et al. (2001). Climate change and forest disturbances. *BioScience*, *51*(9), 723–734.
DeBlander, V., Guyon, J., Hebertson, E., Mathews, K., & Keyes, C. (2012). Utah forest health conditions 2011. *USDA Forest Service Forest Health Protection R4-OFO-report 12-01*.
Dornelas, M. (2010). Disturbance and change in biodiversity. *Philosophical Transactions of the Royal Society Biological Sciences*, *365*, 3719–3727.
Easterling, D. R., Karl, T. R., Gallo, K. P., Robinson, D. A., Trenberth, K. E., & Dai, A. (2000). Observed climate variability and change of relevance to the biosphere. *Journal of Geophysical Research*, *105*(D15), 20101–20114.
Eidenshink, J., Schwind, B., Brewer, K., Zhu, Z., Quayle, B., & Howard, S. (2007). A project for monitoring trends in burn severity. *Fire Ecology Special Issue*, *3*, 3–21.
Frescino, T. S., Patterson, P. L., Freeman, E. A., & Moisen, G. G. (2012). Using FIESTA, an R-based tool for analysts, to look at temporal trends in forest estimates. In R. S. Morin, & G. C. Liknes (Eds.), *Moving from status to trends: Forest inventory and analysis symposium, Baltimore, MD* (pp. 74–78). USDA Forest Service GTR NLTS-P-105.
Gibson, L., Lynam, A. J., Bradshaw, C. J. A., He, F., Bickford, D. P., Woodruff, D. S., et al. (2013). Near-complete extinction of native small mammal fauna 25 years after forest fragmentation. *Science*, *341*, 1508–1510.
Gormanson, D.D., Hansen, M. H., & McRoberts, R. E. (2003). Can a forest/non-forest change map improve the precision of forest area, volume, growth, removals, and mortality estimates? In R. E. McRoberts, G. A. Reams, P. C. Van Deusen, & W. H. McWilliams (Eds.), *Proceedings of the fifth annual forest inventory and analysis symposium, New Orleans, LA* (pp. 75–82). USDA Forest Service GTR WO-69.
Goward, S. N., Masek, J. G., Cohen, W. B., Moisen, G. G., Collatz, J., Healey, S., et al. (2008). Forest disturbance and North American carbon Flux. *EOS Transactions*, *89*(11), 105–106.
Hansen, M. C., & Loveland, T. R. (2012). A review of large area monitoring of land cover change using Landsat data. *Remote Sensing of Environment*, *122*, 66–74.
Hansen, M. C., Potapov, P. V., Moore, R., Hancher, M., Turubanova, A., Tyukavina, A., et al. (2013). High-resolution global maps of 21st-century forest cover change. *Science*, *342*, 850–853.
Harmon, M. E. (2001). Carbon sequestration in forests: Addressing the scale question. *Journal of Forestry*, *4*, 24–29.
Healey, S. P., Lapoint, E., Moisen, G. G., & Powell, S. L. (2011). Maintaining the confidentiality of plot locations by exploiting the low sensitivity of forest structure models to different spectral extraction kernels. *International Journal of Remote Sensing*, *32*(1–2), 287–297.
Healey, S. P., Yang, Z., Cohen, W. B., & Pierce, D. J. (2006). Application of two regression-based methods to estimate the effects of partial harvest on forest structure using Landsat data. *Remote Sensing of Environment*, *101*, 115–126.
Hebertson, E. G., & Jenkins, M. J. (2008). Climate factors associated with historic Spruce Beetle (Coleoptera: Curculionidae) outbreaks in Utah and Colorado. *Environmental Entomology*, *37*(2), 281–292.
Huang, C., Goward, S. N., Masek, J. G., Thomas, N., Zhu, Z., & Vogelmann, J. E. (2010). An automated approach for reconstructing recent forest disturbance history using dense Landsat time series stacks. *Remote Sensing of Environment*, *114*, 183–198.
Intergovernmental Panel on Climate Change (2014). Climate change 2013: The physical science basis. In T. F. Stocker, D. Qin, G. -K. Plattner, M. Tignor, S. K. Allen, J. Boschung, A. Nauels, Y. Xia, V. Bex, & P.M. Midgley (Eds.), *Contribution of Working Group 1 to the fifth assessment report of the Intergovernmental Panel on Climate Change*. Cambridge, UK and New York, NY, USA: Cambridge University Press.
Jin, S., Yang, L., Danielson, P., Homer, C., Fry, J., & Xian, G. (2013). A comprehensive change detection method for updating the National Land Cover Database circa 2011. *Remote Sensing of Environment*, *132*, 159–175.
Kasischke, E. S., Amiro, B.D., Barger, N. N., French, N. H. F., Goetz, S. J., Grosse, G., et al. (2013). Impacts of disturbance on the terrestrial carbon budget of North America. *Journal of Geophysical Research, Biogeosciences*, *118*, 303–316.
Kennedy, R. E., Andréfouët, S., Cohen, W. B., Gómez, C., Griffiths, P., Hais, M., et al. (2014). Bringing and ecological view of change to Landsat-based remote sensing. *Frontiers in Ecology and the Environment (e-view)*, http://dx.doi.org/10.1890/130066.
Kennedy, R. E., Cohen, W. B., & Schroeder, T. A. (2007). Trajectory-based change detection for automated characterization of forest disturbance dynamics. *Remote Sensing of Environment*, *110*, 370–386.
Kennedy, R. E., Yang, Z., & Cohen, W. B. (2010). Detecting trends in forest disturbance and recovery using yearly Landsat time series: 1. LandTrendr — Temporal segmentation algorithms. *Remote Sensing of Environment*, *114*, 2897–2910.
Loveland, T. R., & Dwyer, J. L. (2012). Landsat: Building a strong future. *Remote Sensing of Environment*, *122*, 22–29.
Man, G. (2012). Major forest insect and disease conditions in the United States: 2011. *USDA Forest Service Forest Health Protection Report FS-1110*.
Masek, J. G., Goward, S. N., Kennedy, R. E., Cohen, W. B., Moisen, G. G., Schleeweis, K., et al. (2013). United States forest disturbance trends observed using Landsat time series. *Ecosystems*, *16*, 1087–1104.
McRoberts, R. E., Holden, G. R., Nelson, M.D., Liknes, G. C., & Gormanson, D.D. (2006). Using satellite imagery as ancillary data for increasing precision of estimates for the Forest Inventory and Analysis Program of the USDA Forest Service. *Canadian Journal of Forest Research*, *36*, 2968–2980.
McRoberts, R. E., & Tomppo, E. O. (2007). Remote sensing support for national forest inventories. *Remote Sensing of Environment*, *110*, 412–419.
McRoberts, R. E., Tomppo, E. O., & N sset, E. (2010). Advances and emerging issues in national forest inventories. *Scandinavian Journal of Forest Research*, *25*, 368–381.
McRoberts, R. E., & Walters, B. F. (2012). Statistical inference for remote sensing-based estimates of net deforestation. *Remote Sensing of Environment*, *124*, 394–401.
McRoberts, R. E., Wendt, D.G., & Liknes, G. C. (2005). Stratified estimation of forest inventory variables using spatially summarized stratifications. *Silva Fennica*, *39*(4), 559–571.
Meigs, G. W., Kennedy, R. E., & Cohen, W. B. (2011). A Landsat time series approach to characterize bark beetle and defoliator impacts on tree mortality and surface fuels in conifer forests. *Remote Sensing of Environment*, *115*, 3707–3718.
Nelson, M.D., McRoberts, R. E., Holden, G. R., & Bauer, M. E. (2009). Effects of satellite image spatial aggregation and resolution on estimates of forest land area. *International Journal of Remote Sensing*, *30*(8), 1913–1940.
Nelson, M.D., McRoberts, R. E., Liknes, G. C., & Holden, G. R. (2002). Comparing forest/non-forest classifications of Landsat TM imagery for stratifying FIA estimates of forest land area. In R. E. McRoberts, G. A. Reams, P. C. Van Deusen, & W. H. McWilliams (Eds.), *Proceedings of the fourth annual forest inventory and analysis symposium, New Orleans, LA* (pp. 121–182). USDA Forest Service GTR NC-252.
O'Halloran, T. L., Law, B. E., Goulden, M. L., Zhuosen, W., Barr, J. G., Schaaf, C., et al. (2011). Radiative forcing of natural forest disturbances. *Global Change Biology*, http://dx.doi.org/10.1111/j.1365-2486.2011.02577.x.
Olofsson, P., Foody, G. M., Stehman, S. V., & Woodcock, C. E. (2013). Making better use of accuracy data in land change studies: Estimating accuracy and area and quantifying uncertainty using stratified estimation. *Remote Sensing of Environment*, *129*, 122–131.
Patterson, P. L., & Finco, M. (2011). Calculation of upper confidence bounds on proportion of area containing not-sampled vegetation types: An application to map unit definition for existing vegetation maps. *Mathematical and Computational Forestry & Natural-Resource Sciences*, *3*(2), 98–101.
Plugmacher, D., Cohen, W. B., Kennedy, R. E., & Yang, Z. (2014). Using Landsat-derived disturbance and recovery history and lidar to map forest biomass dynamics. *Remote Sensing of Environment*, *151*, 124–137.
Pollard, J. E., Westfall, J. A., Patterson, P. L., Gartner, D. L., Hansen, M., & Kuegler, O. (2006). Forest inventory and analysis national data quality assessment report for 2000 to 2003. In U.S. Department of Agriculture (Ed.), Fort Collins, CO: Rocky Mountain Research Station (43 pp.).
Raftery, A. E., Li, N., Ševčiková, H., Gerland, P., & Heilig, G. K. (2012). Bayesian probabilistic population projections for all countries. *Proceedings of the National Academy of Sciences*, *109*(35), 13915–13921.
Reams, G. A., Smith, W. D., Hansen, M. H., Bechtold, W. A., Roesch, F. A., & Moisen, G. G. (2005). The forest inventory and analysis sampling frame. In W. A. Bechtold, & P. L. Patterson (Eds.), *The enhanced Forest Inventory and Analysis program — National sampling design and estimation procedures*. USDA Forest Service GTR SLTS-80.
Ruefenacht, B., Finco, M. V., Nelson, M.D., Czaplewski, R., Helmer, E. H., Blackard, J. A., et al. (2008). Conterminous U.S. and Alaska forest type mapping using Forest Inventory and Analysis data. *Photogrammetric Engineering and Remote Sensing*, *74*(11), 1379–1388.
Schroeder, T. A., Wulder, M.A., Healey, S. P., & Moisen, G. G. (2012). Mapping wildfire and clearcut harvest disturbances in boreal forests with Landsat time series data. *Remote Sensing of Environment*, *115*, 1421–1433.
Scott, C. T., Bechtold, W. A., Reams, G. A., Smith, W. D., Westfall, J. A., Hansen, M. H., et al. (2005). Sample-based estimators used by the forest inventory and analysis national information management system. In W. A. Bechtold, & P. L. Patterson (Eds.), *The enhanced Forest Inventory and Analysis program — National sampling design and estimation procedures*. USDA Forest Service GTR SLTS-80.
van Mantgem, P. J., Stephenson, N. L., Byrne, J. C., Daniels, L. D., Franklin, J. F., Fulé, P. Z., et al. (2009). Widespread increase of tree mortality rates in the Western United States. *Science*, *323*(5913), 521–524.
Vogelmann, J. E., Kost, J. R., Tolk, B., Howard, S., Short, K., Chen, X., et al. (2011). Monitoring landscape change for LANDFIRE using multi-temporal satellite imagery and Ancillary data. *IEEE Journal of Selected Topics in Applied Earth Observations and Remote Sensing*, *4*, 252–264.
Vogelmann, J. E., Xian, G., Homer, C., & Tolk, B. (2012). Monitoring gradual ecosystem change using Landsat time series analyses: Case studies in selected forest and rangeland ecosystems. *Remote Sensing of Environment*, *122*, 92–105.
Weed, A. S., Ayres, M. P., & Hicke, J. (2013). Consequences of climate change for biotic disturbances in North American forests. *Ecological Monographs*, *83*(4), 441–470.
Westerling, A. L., Hidalgo, H. G., Cayan, D. R., & Swetnam, T. W. (2006). Warming and earlier Spring increase western U.S. forest wildfire activity. *Science*, *313*, 940–943.
Wulder, M.A., Masek, J. G., Cohen, W. B., Loveland, T. R., & Woodcock, C. E. (2012). Opening the archive: How free data has enabled the science and monitoring promise of Landsat. *Remote Sensing of Environment*, *122*, 2–10.
Zhu, Z., Woodcock, C. E., & Olofsson, P. (2012). Continuous monitoring of forest disturbance using all available Landsat imagery. *Remote Sensing of Environment*, *122*, 75–91.